The shape of sunspots and activity cycles

Andrey Tlatov (tlatov@mail.ru)
Pulkovo Observatory

Research Article

Keywords: Sunspots, solar cycle, solar activities

Posted Date: May 12th, 2022

DOI: https://doi.org/10.21203/rs.3.rs-1633066/v1

Solar Physics
DOI: 10.1007/•••••-•••-•••-••••-•

The Shape of Sunspots and Solar Activity Cycles

Andrey G. Tlatov[1]••

Abstract
The paper presents the results of the analysis of the geometric characteristics of sunspots for the period of 15-24 cycles of activity according to the data of Kislovodsk (1956-2021) and RGO (1918-1972) Observatories. To study the shape of sunspots, we used the method of obtaining the average density of the distribution, as well as the average values of the ratio of the extent of the sunspots in latitude and longitude. The deviation of the shape of sunspots from the axisymmetric configuration is investigated. It was found that the sunspots, as a rule, have an ellipsoid shape, and the major axis of the ellipse, as a rule, is elongated along longitude and has a predominant slope to the equator, different in the Northern and Southern hemispheres.
The relationship between the shape of sunspots in the current cycle and the amplitude of the next cycle of activity is found. The greater the elongation of the sunspots along the longitude in the current cycle, the more powerful the next cycle of activity will be.

Keywords: Sunspots — solar cycle — solar activities

1. Introduction

Archival photographic images of the Solar photosphere according to various observatories and modern observations allow us to study in detail the structure and fine structure of sunspots as one of the most remarkable manifestations of solar activity. Ever since the first systematic observations of the Sun's disk, which can be attributed to the 18th century, astronomers have sought not just to take into account the number of sunspots on a given day, but to make as detailed sketches of the shape of the sunspots as possible, thereby emphasizing the diversity of their manifestations (see for example (Carrington, 1863)). Later,

A.G. Tlatov
tlatov@mail.ru

[1] Kislovodsk Mountain Astronomical Station of the Pulkovo observatory,Kislovodsk, Gagarina str. 100, 357700, Russia.

this knowledge formed the basis of the classification system of sunspots and sunspot groups, used in various modifications to this day.

At the same time, a wide range of issues continues to be debatable. It is generally assumed that the sunspots formed at the places where strong magnetic fields enter the photosphere are located slightly below the outer boundary of the photosphere and represent certain depressions in its surface. This conclusion is based on both theoretical models of spot formation and projection effects observed when sunspots move across the Sun's disk. One of these effects is called the Wilson effect and consists in changing the visible part of the spot when it is observed at different angles (in the center of the disk or near the limb) (Wilson, 1965). Further studies have shown that the manifestations of the Wilson effect have differences in the eastern and western hemispheres (Obashev et al., 1982; Collados et al., 1987). To study the features of the shape of sunspots, it is useful to have an idea of how a spot looks on average and its typical parameters (Bray and Loughhead, 1962).

In (Illarionov and Tlatov, 2016) a method was proposed for studying the average profile of a spot on a disk by scaling and superimposing images of all sunspots and constructing a histogram of the brightness distribution of the combined image. It was shown that the average shape of sunspots has a teardrop shape and is elongated in the longitude direction.

In this paper, we have analyzed the shapes of sunspots according to the processing of photoheliograms from the archive of the Kislovodsk Mountain Astronomical Station (KMAS) for the period 1956-2021 and the photographic archive of observations of the RGO Observatory in the period 1918-1972.

2. Data and Processing Methods

2.1. Observational Data

The Kislovodsk Mountain Astronomical Station has been performing daily observations of sunspots since 1948. During this time, a large archive of photographic plates (1948-2010) and digital images (2010- present) of the solar photosphere has been accumulated.

We digitized photographic plates, which made it possible to reconstruct the activity of sunspots using computer recognition methods (Tlatov et al., 2014). Digitization data from 1956 are presented on the website https://observethesun.ru. In total, according to Kislovodsk data, the characteristics of $\approx 82 \cdot 10^3$ groups and $\approx 340 \cdot 10^3$ individual sunspots were obtained. Figure 1 shows a time-latitude diagram of the position of sunspot groups, and the separation lines of activity cycles. Cycle boundaries were selected visually on the latitude-time diagram. The separation of sunspots into groups was carried out in accordance with the data on the characteristics of the groups of sunspots presented in the catalog https://http://158.250.29.123:8000/web/Soln_Dann/.

Another data set used by us were Royal Greenwich Observatory (RGO) photographic plates in the period from 1918 to 1972 (Tlatov et al., 2016). The archive included photographic plates of observations conducted at the Royal Observatory

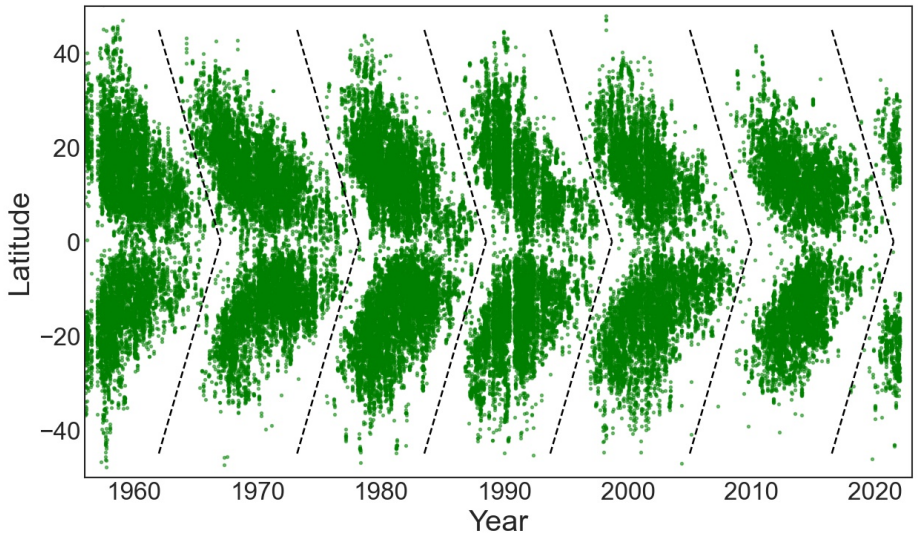

Figure 1. The time-latitude diagram of the distribution of groups of sunspots according to KMAS data. Dotted lines represent the sections of the cycle boundaries.

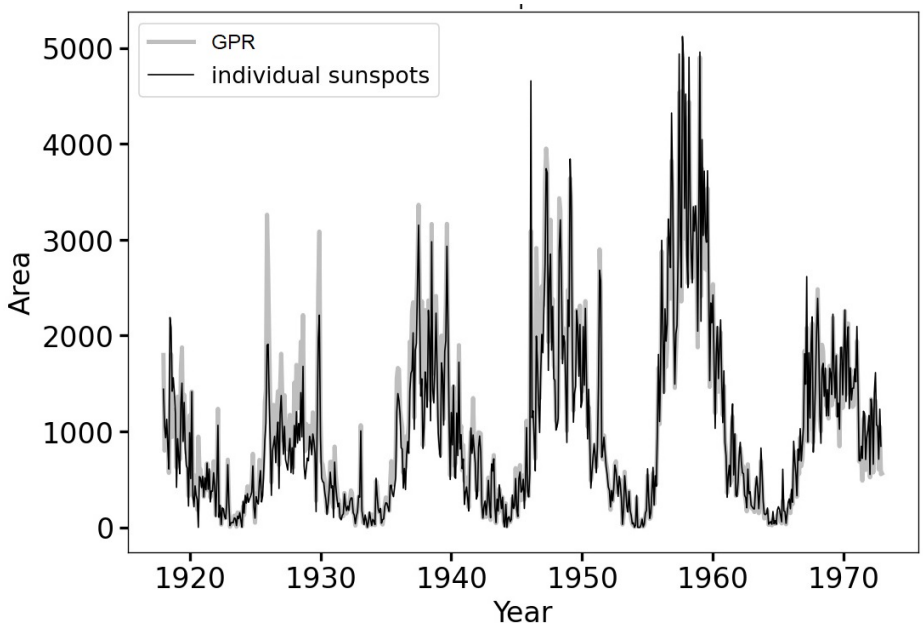

Figure 2. Comparison of the new measures individual sunspots area by RGO observation and manual measurements Greenwich Photo-heliographic Results (GPR) in millionths of hemisphere (μhs).

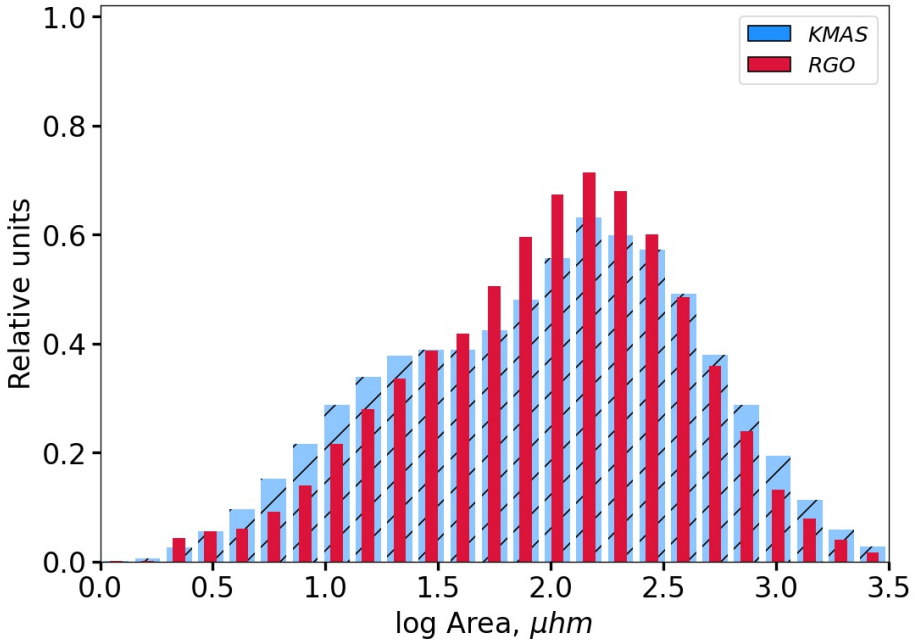

Figure 3. Histogram of the distribution of the area of sunspots according to KMAS and RGO data.

of Greenwich, the Cape of Good Hope Observatory, the Kodaikanal Observatory and some others. In total, the RGO archive available to us contains about 26,000 thousand records. The images were digitized with a resolution of 16 bits, and the radius of the Sun was about 1600 pixels. The RGO data was processed only in automatic mode. A total of $\approx 78.7 \cdot 10^3$ groups and $\approx 231 \cdot 10^3$ individual sunspots were identified. Figure 2 shows a comparison of the area of sunspots according to our processing data and the area according to Greenwich Photoheliographic Results (GPR) (http://solarcyclescience.com/activeregions.html). The correlation between the two sets was $r \approx 0.974$. At the same time, according to the semi-automatic processing of KMAS, an average of $\approx 5,144$ sunspots are allocated per year, and according to the fully automatic processing of RGO, on average there are $\approx 4,200$ sunspots per year. This is due to the difficulty in processing fully automatic confident identification of small sunspots and sunspots near the limb. Differences in the distribution of sunspots by area according to RGO and KMAS data are shown in Figure 3.

2.2. Shape of Sunspots

During processing, we cataloged not only tabular information, such as coordinates, area, group membership, but also information about the configuration of the shape of sunspots. This allows you to analyze the configurations of the shape of sunspots. Also, the representation of geometric information allows you to visually assess the level of solar activity, the relative location of solar activity, and their geo-efficiency in the case of flare and eruptive processes.

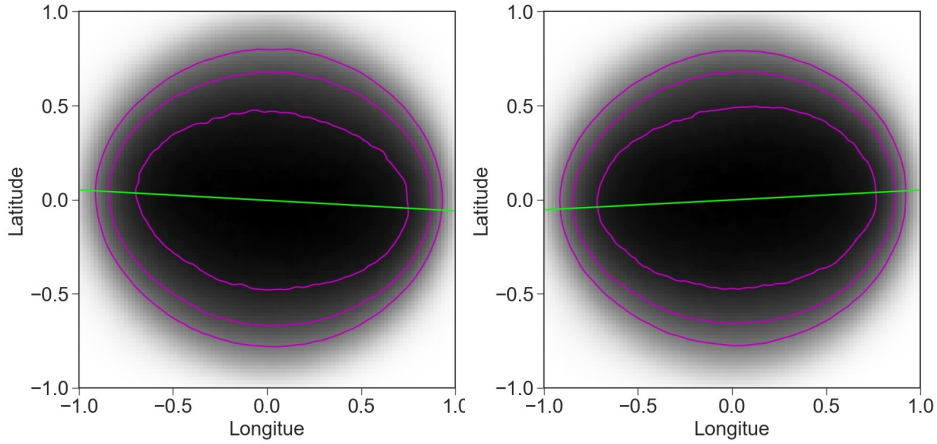

Figure 4. The shape of sunspots in the Northern (left) and Southern (right) hemispheres according to Kislovodsk data processing 1956-2021.

To analyze the shape, we considered the location of the photosphere-penumbra boundary. We selected sunspots with an area of $S > 30$ μhm and at a distance of $r/R_{\odot} > 0.7$. This choice of area is related to selecting sunspots with sufficiently developed umbra (Tlatov and Pevtsov, 2014).

To determine the direction of elongation, there are a number of approaches, from which the least squares method and the contour method can be distinguished. In the contour method used in this work, the asymmetry of isodensit in the distribution density matrix is investigated. To exclude the influence of projection effects, the direction of the elongation of the spot is determined not in flat, but in spherical coordinates. To do this, we translated the pixels of the image into heliographic coordinates, taking into account the angles P and B. Then, similarly to (Illarionov and Tlatov, 2016), the image is scaled in such a way that the spot is written off into a single circle with the center coinciding with the center of the spot. All the resulting images are superimposed on each other, and a histogram of the brightness distribution is built based on these.

Figure 4 shows the distribution density of the average profile of sunspots. The red lines show the contours of the isolines for the distribution density for the value $k = (1.0, 1.3, 1.6) \cdot Av$, where Av is the average value of the distribution. The green line represents the direction of the major axis of the ellipse inscribed for the intensity isolines $1.3 \cdot Av$.

We can note that the major axis of the ellipse has an inclination with the solar equator, such that the eastern parts of the sunspots are further away from the equator than the western ones. Thus, for the Northern and Southern hemispheres, they have an inclination with respect to the equator in the same direction as the axes of the bipolar sunspot groups. At the same time, we could not establish a clear change in the angle of inclination of the sunspots from latitude, similar to Joy's law (Hale et al., 1919). Consider the parameter characterizing the elongation of the shape of the spot $e = b/a$, where b and a are the minor and major axes of the inscribed ellipse. In the future, we will use this

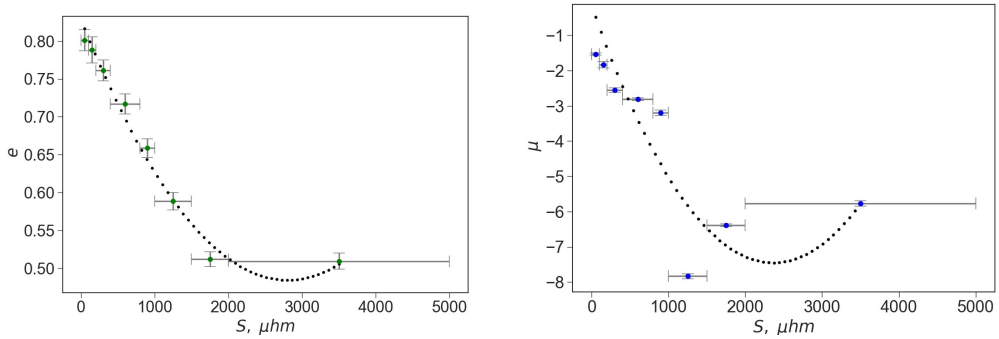

Figure 5. Change of the parameter of oblateness $e = b/a$ (Left) and the angle of inclination of the axis of the sunspots μ (Right).

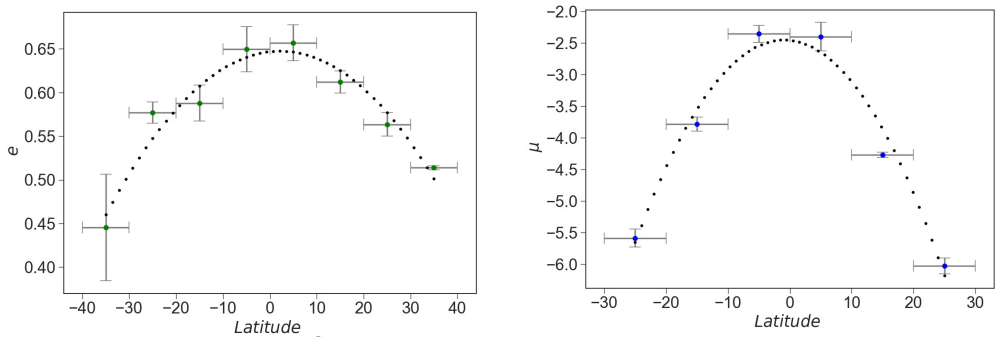

Figure 6. Variation of the parameter e (Left) and the angle of inclination of the axis of sunspots μ (Right) from latitude.

definition of the parameter e, even for sunspots where the latitude size is greater than the longitude size. Basically, we will calculate this parameter for intensity values $1.3 \cdot Av$, but the conclusions are valid for a wide range of variation of the parameter k. In Figure 4 , the parameter values for different hemispheres were $e_N = 0.783$ and $e_S = 0.778$.

Parameter e depends on the area of the sunspots (Figure 5 , Left). For sunspots of small and medium area, the parameter e decreases with increasing area, which corresponds to an increase in the oblateness of the sunspots in the direction of latitude. But for large sunspots $S > 2500$ μhm, the parameter e ceases to change significantly and even an increase in values is observed. The change of the angle μ from the area is also not unambiguous.The greatest angle of μ is achieved for sunspots with an area of ≈ 1000 μhm (Figure 5, Right).

Parameter e varies from latitude (Figure 6), reaching a maximum near the equator. At the same time, we must take into account that at high latitudes for round sunspots, the distance in longitude, expressed in meters, is less at high latitudes than near the equator. Taking into account this correction, for round sunspots, the parameter e should increase with latitude.

The oblateness of sunspots can be estimated by a simpler method, for example, using the ratio of the size of the sunspots in latitude $\Delta\theta$ to the size in

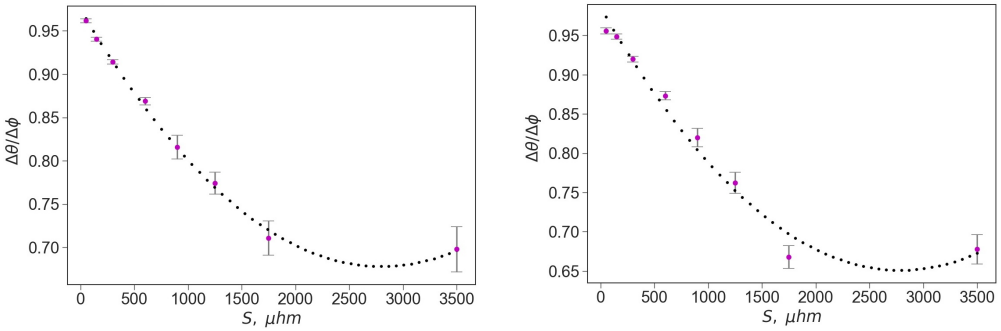

Figure 7. Change of the parameter $rat = \Delta\theta/\Delta\phi$ from the sunspot area according to RGO (left) and KMAS (right) data.

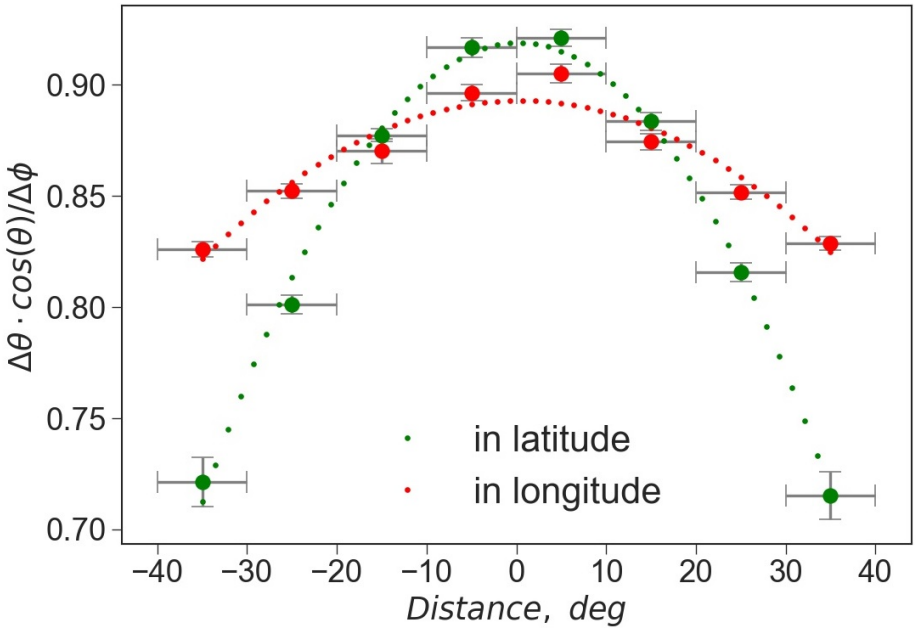

Figure 8. Change in the parameter *rat* in latitude and longitude.

longitude $\Delta\phi$. We introduce the $rat = \Delta\theta \cdot cos(\theta')/\Delta\phi$, where θ' is the latitude taken taking into account the heliographic angle B.

As well as for e parameter, the *rat* parameter shows an increase in the oblateness of sunspots with an increase in the area of sunspots. Figure 7 shows the change of the rat parameter depending on the area of sunspots for RGO and KMAS. The dependence can be approximated by a quadratic dependence, but the linear dependence is also well suited for small and medium sunspots $rat_{RGO} = 0.92 - 7.98 \cdot 10^{-5} \cdot S$. For KMAS data, this ratio can be written as $rat_{KMAS} = 0.92 - 8.96 \cdot 10^{-5} \cdot S$.

The *rat* parameter varies significantly in latitude and less intensively in longitude (Figure 8). To construct this dependence, we used restrictions of $\pm 30^o$

in longitude from the central meridian for the dependence of $rat(\theta)$ in latitude, and for $\pm 30^o$ from the equator for the dependence on longitude $rat(\phi)$. Figure 8 shows that the dependence on latitude is stronger than on longitude, therefore, the oblateness of the sunspots in longitude cannot be explained by the Wilson effect, which depends on the distance from the center of the disk.

2.3. The Shape of Sunspots and Activity Cycles

Consider the change in the shape of sunspots depending on the amplitude of solar activity cycles. To do this, we will average the shape of sunspots with an area of more than $S > 30$ μhm and spaced from the limb at a distance of less than $r/R_\odot > 0.7$. We found that the shape of sunspots is related to the amplitude of the next cycle of activity.

Figure 9 shows the values of parameter e measured in cycles 19-24 and the amplitudes of the next activity cycle. The amplitudes of the activity cycles SN were taken for the new version of the spot index (Usoskin et al., 2014). For cycle 25, we took the value $SN_{25} = 110$, since this value lies on the regression line (Figure 9). The dependence of the amplitude SN on the value e for cycles n is expressed by $SN_n = 948.01(\pm 102) - 1025.5(\pm 135) \cdot e_{n-1}$ at correlation $r = 0.96$.

A significant relationship between the parameter of the shape of the sunspots e_{n-1} and the amplitude of the next cycle of SN_n activity exists not only for the maximum sunspots in the group, but, for example, for the second for the area of the sunspots. The correlation turned out to be less than for the maximum sunspots in the group $r = 0.93$, but also quite high.

To verify the relationship between the shape of the sunspots and the amplitude of the cycles, we can also use the rat parameter. Figure 10 shows the rat parameters averaged over the cycle for the maximum sunspots according to RGO and KMAS data. The correlation coefficient of the rat_{n-1} coupling with the amplitude of the SN_n cycles turned out to be quite high for RGO $r \approx 0.86$ data and KMAS $r \approx 0.84$ data.

From the RGO and KMAS data, we can compile a summary of the characteristics of individual sunspots. Figure 11 shows the regression between the parameter e in the cycle and the amplitude of the subsequent activity cycle, calculated for the maximum sunspots in the activity groups for cycles 15-24. The characteristics of the sunspots were taken according to RGO data before 1956 and KMAS observations after that date. The parameter was calculated for sunspots of maximum area in solar groups. In contrast to the calculations in Figure 9 , the distribution density was calculated by a weight depending on the area of sunspots. The correlation coefficient was $r \approx 0.82$.

3. Discussion

The shape of sunspots on average differs from the regular round shape. The sunspots are elongated along the direction of longitude and correspondingly compressed along latitude (Figure 4). This effect cannot be explained only by the Wilson effect associated with the dipping of sunspots below the level of the

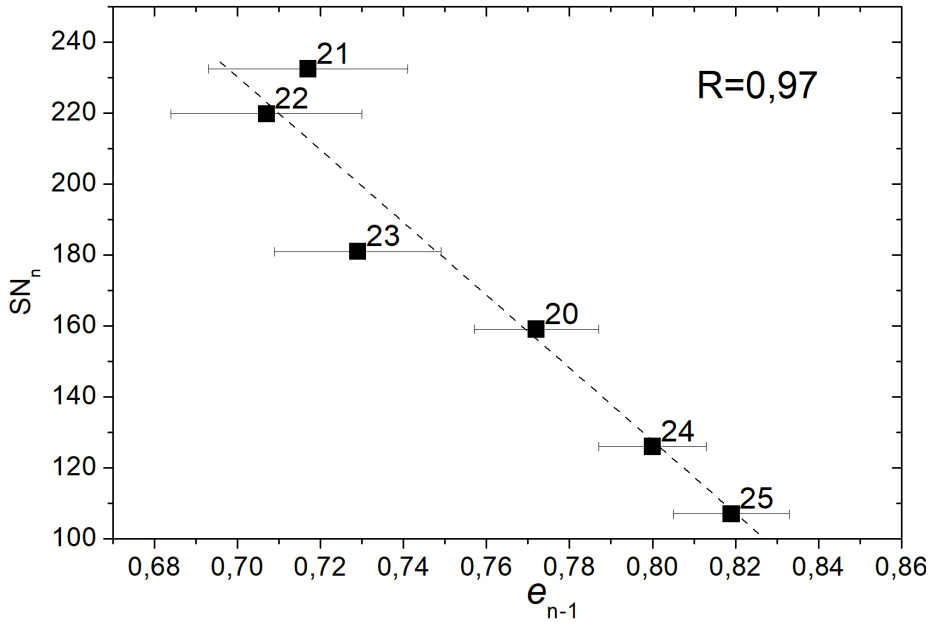

Figure 9. The relationship of the solar activity cycle of the subsequent SN_n activity cycle on the shape parameter of the sunspots e_{n-1}. The parameter e was calculated for the maximum sunspots in the group in terms of area. The error of determining the value of e is presented. For cycle 25, we took the value $SN_{25} = 110$.

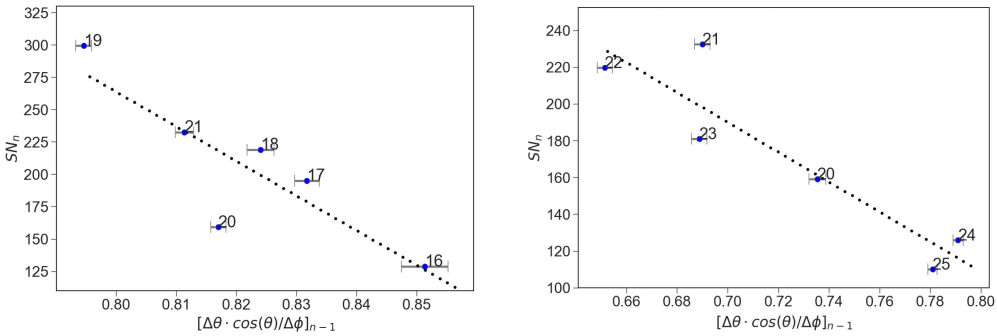

Figure 10. The dependence of the amplitude of the activity cycles on the parameter of the sunspots $rat = \Delta\theta/\Delta\phi$ in the previous cycle of activity according to the processing data of RGO (Left) and KMAS (Right).

quiet photosphere (Wilson, 1965). The Wilson effect appears near the limb, but as shown in Figure 7, this is not always the case.

Also, for sunspots, there is a small angle at which the eastern parts of the sunspots are farther from the equator than the western regions. This may indicate the effect of differential rotation on the sunspots. Indeed, with differential rotation, the high-latitude parts of the sunspots will shift relative to the low-latitude parts. With this shift, the angle of inclination of the axis of the sunspots

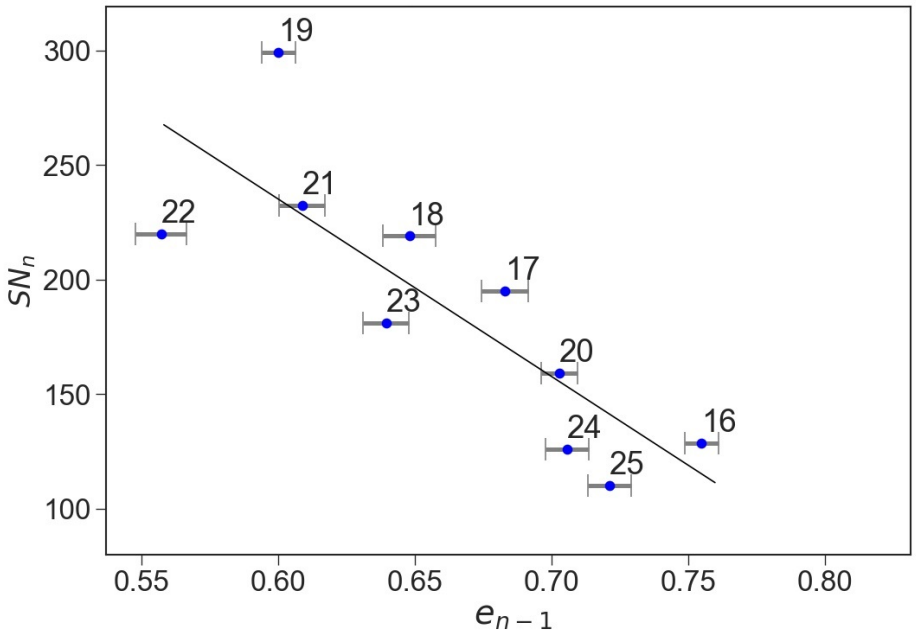

Figure 11. The relationship between the parameter e_{n-1} and the amplitude of the next cycle of activity SN_n according to the summary series RGO and Kislovodsk of individual sunspots for the period 1918-2021.

will appear. For sunspots, the amount of flattening of the sunspots e or rat depends on the area of the sunspots (Figure 5,Figure 7). For the angle of inclination μ, this dependence is not so obvious. The angle μ increases in absolute magnitude for sunspots in the range $S < 1000$ μhm, but then decreases.

Thus, by measuring the deviations of the shape of the sunspots from the round shape, we can study the differential rotation of the Sun. The detection of a connection between the shapes of sunspots and the amplitude of the next cycles of activity (Figure 8 -11) may indicate a change in the rotation speed from cycle to cycle.

Indeed, if we construct linear approximations of the change for different cycles n for sunspots of different areas, then we can see changes in the slope angles of the dependence $rat_n = fn(S) \approx a_n + b_n \cdot S$ (Figure 12). In this case, the b_{n-1} coefficient is associated with the amplitude of the subsequent SN_n cycle with a correlation coefficient $r \approx 0.76$. The more compressed the sunspots are in the current cycle, the greater the amplitude of the next cycle of activity.

The shape of sunspots depends on the area S (Figure 7). Perhaps this is due to the lifetime of the sunspots. The larger the sunspots, the longer their lifetime (Gnevyshev, 1938) and the longer the time they are affected by differential rotation, changing their shape. But in this case, we can reconstruct the shape of the sunspots from the area, and then estimate the amplitude of the activity cycles. Indeed, let's take the most famous number of areas of groups of sunspots (http://solarcyclescience.com/activeregions.html) for cycles

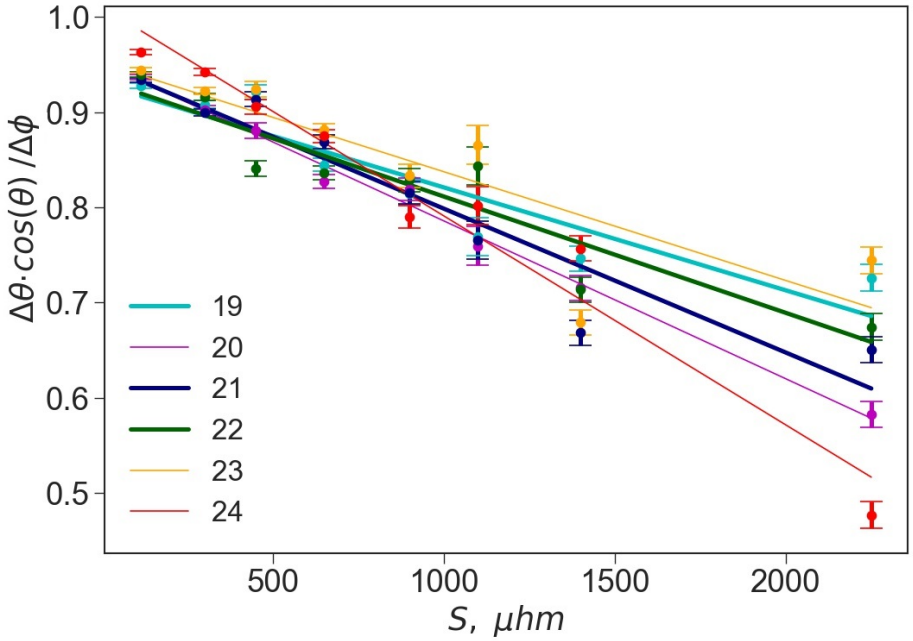

Figure 12. Linear regressions between the rat_n value and the area for cycles $n = 19 - 24$ according to KMAS data.

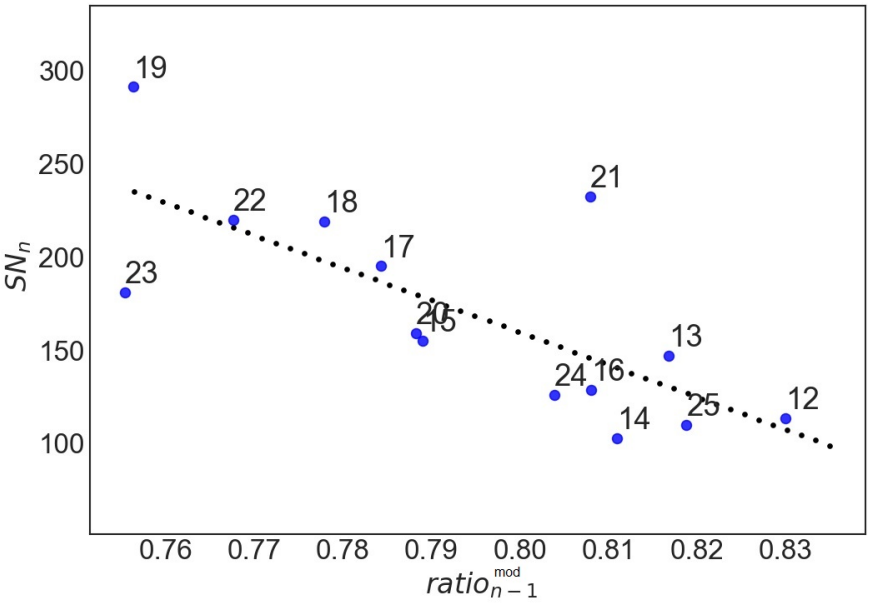

Figure 13. Modeling of the parameter of the shape of sunspots according to the areas of sunspot groups GPR and the amplitude of the next cycle of activity.

$n = 11 - 24$ and calculate the average shape of the spot, using the ratio for $rat^{mod} = f(S) = a + b \cdot S$. Then we get the average value of the parameter $rat_n^{mod} = (\sum f(S) \cdot S / \sum S)_n$, in cycles of activity and is comparable to the amplitude of the following cycles of activity $n+1$. Figure 13 shows this ratio for parameters $a = 0.97$ and $b = 3.9 \cdot 10^{-4}$. The correlation coefficient turned out to be quite large $r \approx 0.74$. Consider the difference for cycles 18 and 19. Despite the fact that the average area of the spot groups in Cycle 19 was slightly larger than in Cycle 18 $S_{19}^{avr} = 205.9$ μhm and $S_{18}^{avr} = 200.1$ μhm, the median values of the areas in cycle 18 were larger than in cycle 18: $S_{19}^{med} = 93$ μhm and $S_{18}^{med} = 95$ μhm. When obtaining this regression, we did not use information about the shape of the sunspots, but only data on the areas of the groups, in fact, calculating the ratio $(\sum S^2 / \sum S)_n$ in the activity cycles and comparing it with the amplitude of the next activity cycle. This may indicate that sunspots of different areas are involved in the formation of conditions for the generation of new activity cycles in different ways.

4. Conclusions

The performed analysis established new properties in the geometry of sunspots. The method of averaging the shape of sunspots over a long period showed that sunspots differ from the round shape and, as a rule, are elongated along the longitude. Also, sunspots have an inclination with respect to the solar equator. The eastern parts of the sunspots are located farther from the equator than the western ones. This is similar to the angle of the sunspot bipoles.

The most likely mechanism for the formation of elongated sunspots may be differential rotation in latitude. Indeed, in this case, the high-latitude parts of the sunspots will shift to the east, and the low-latitude ones to the west. In this case, the shape of the sunspots will stretch in a direction parallel to the equator, and the long axis of the sunspots will have a slope with respect to the equator. That is, to have a shape similar to Figure 3. Thus, the study of the shape of sunspots can help in the study of variations in the differential rotation of the solar atmosphere.

To study the shape of the sunspots, we used the method of averaging over many sunspots during the cycle. One of the methods was the method of inscribing an ellipse into an average density matrix. Another method was to average the ratio of the latitude and longitude extent of the sunspots.

It was found that the shape of sunspots averaged over a cycle is related to the amplitude of the next cycle of activity. The more elongated the sunspots are along the longitude, the more powerful the next cycle of activity will be.

The oblateness of the sunspots in the first approximation is linearly related to the area (Figure 7). This is probably due to the lifetime of the sunspots (Gnevyshev, 1938) and the length of exposure to differential rotation on these sunspots. It is possible that the differential rotation varies from cycle to cycle (Figure 3), which leads to a change in the amplitudes of solar activity.

References

Brown, M., Canfield, R., Pevtsov, A.: 1999, Magnetic Helicity in Space and Laboratory Plasmas, Geophys. Mon. Ser. 111, AGU. doi: 10.1029/GM111

Bray, R. J., Loughhead, R.E. : 1962, Australian Journal of Physics, 15, 482. doi: 10.1071/PH620482

Carrington, R.: 1863, Observations of the spots on the Sun from November 9 1853 to march 24 1861, (G. Nokman, printer, Maiden Lane, Covert Garden, London)

Collados, M., del Toro Iniesta, J.C., Vazquez, M.A. : 1987, *Solar Phys.*, 112, 281. doi: 10.1007/BF00148782

Gnevyshev, M. N. : 1938 Izvestiya Glavnoj Astronomicheskoj Observatorii v Pulkove, 16 36.

Hale, G.E., Ellerman, F., Nicholson, S.B., Joy, A.H.: 1919, *Astrophys. J.*, 49, 153. doi: 10.1086/142452

Illarionov, E.A., Tlatov, A.G.: 2016, Geomagnetism and Aeronomy, 56, 1031. doi: 10.1134/S0016793216080089

Obashev, S.O., Gainullina, R.K., Minasiants, T.M., Minasiants, G.S.: 1982, *Solar Phys.*, 78, 59. doi: 10.1007/BF00151142

Tlatov, A. G., Skorbehz, N. N., Ershov, V. N.: 2016, ASP Conference Series, 504, 237

Tlatov, A. G., Pevtsov, A. A.: 2014, *Solar Phys.*, 289, 1143. doi: 10.1007/s11207-013-0382-9

Tlatov, A.G., Vasil'eva, V.V., Makarova, V.V., Otkidychev, P.A.: 2014, *Solar Phys.*, 289, 1403. doi: 10.1007/s11207-013-0404-7

Usoskin, I., Kovaltsov, G., Kiviaho, W.R.: 2021, *Solar Phys.*, 296, article id.13. doi: 10.1007/s11207-020-01750-9

Wilson, P.R.: 1965, *Astrophys. J.*, 142, 773. doi: 10.1086/148338